JACS
JOURNAL OF THE AMERICAN CHEMICAL SOCIETY

Communication

pubs.acs.org/JACS

NanoCluster Beacons Enable Detection of a Single N^6-Methyladenine

Yu-An Chen,[†] Judy M. Obliosca,[†] Yen-Liang Liu, Cong Liu, Mary L. Gwozdz, and Hsin-Chih Yeh*

Department of Biomedical Engineering, Cockrell School of Engineering, University of Texas at Austin, Austin, Texas 78712, United States

Supporting Information

ABSTRACT: While N^6-methyladenine (m^6A) is a common modification in prokaryotic and lower eukaryotic genomes and has many biological functions, there is no simple and cost-effective way to identify a single N^6-methyladenine in a nucleic acid target. Here we introduce a robust, simple, enzyme-free and hybridization-based method using a new silver cluster probe, termed methyladenine-specific NanoCluster Beacon (maNCB), which can detect single m^6A in DNA targets based on the fluorescence emission spectra of silver clusters. Not only can maNCB identify m^6A at the single-base level but it also can quantify the extent of adenine methylation in heterogeneous samples. Our method is superior to high-resolution melting analysis as we can pinpoint the location of m^6A in the target.

The number of nucleic acid modifications identified in the genomes and transcriptomes has exploded since the first discovery of noncanonical nucleobases six decades ago.[1,2] Many of the modifications in genomes are heritable epigenetic marks that influence the way the genes are expressed and eventually define cell status among the higher organisms.[3] In particular, N^6-methyladenine (m^6A; denoted as A* in Figures 1−4) is a methylation modification abundant in prokaryotic genomes[4] and also found in lower eukaryotes[5,6] and higher plants.[7] While the biological functions of m^6A at GATC sites in single-celled organisms are well studied (such as genome defense, mismatch repair, and gene expression control[8]), its roles in eukaryotic genomes remain largely unknown.[6] This is partly due to the fact that detection of m^6A at specific sites in a sequence is challenging. So far detection of N^6-methyladenine in DNA has been demonstrated using a single-molecule, real-time sequencing method.[9,10] Detection of N^6-methyladenosine in RNA has been shown using (1) nuclease cleavage followed by thin-layer chromatography (TLC) or mass spectrometry (MS),[11] (2) immunocapturing of m^6A-containing RNA fragments followed by sequencing,[12] (3) ligation,[13] and (4) a selective polymerase.[14] However, these methods are laborious (e.g., require multiple steps to identify a single site), time-consuming (e.g., TLC and MS), and high-cost (e.g., enzymatic reaction). Whereas high-resolution melting (HRM) analysis[15] is able to detect a single m^6A modification within a target DNA via the destabilizing effect of m^6A, HRM cannot pinpoint the location of m^6A in the sequence. A simple and cost-effective way to identify single m^6A at any specific sites is therefore highly desired.

Here we introduce a robust, simple, enzyme-free and hybridization-based method for m^6A detection with pinpoint specificity, using a new type of silver cluster-based DNA probe, which we term methyladenine-specific NanoCluster Beacon (maNCB). Yeh and co-workers have previously introduced NanoCluster Beacon (NCB) that fluoresces upon binding to a DNA target.[16−19] NCBs employ DNA-templated, few-atom silver nanoclusters (DNA/Ag NCs, about 2−20 silver atoms per cluster[20]) as reporters whose fluorescence can be significantly enhanced through interactions with a nearby G-rich sequence (called an enhancer).[16,17] Not only is the fluorescence of silver clusters activated, but the fluorescence color can also respond to the "alignment" of silver cluster with respect to the enhancer

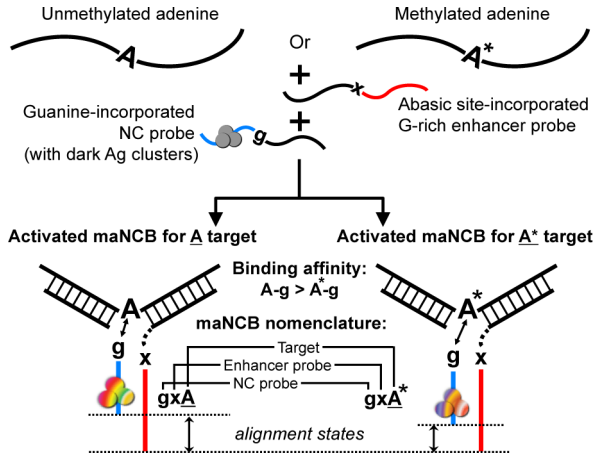

Figure 1. N^6-Methyladenine detection using methyladenine-specific NanoCluster Beacons (maNCBs) (not drawn to scale). Consisting of an NC probe (i.e., the cytosine-rich Ag cluster-nucleation sequence shown in blue) and an enhancer probe (i.e., the guanine-rich sequence shown in red), maNCB forms two 3-way junctions (3WJ) when hybridizing with the two targets (A target or A* target; A* represents m^6A). Here only the nucleotides-of-interest (**A*** or **A**) on the two targets and the recognition nucleotides on the two probes (**g** or **x**) are shown. The nomenclatures that represent the two resulting probe-target hybridization complexes are **gxA** and **gxA***, respectively. The lowercase letters, **g** and **x**, indicate the recognition nucleotides on the NC and the enhancer probes, respectively. The capital letter represents the type of adenine on the target. Here **x**, the abasic site, serves as a noninteracting, neutral site, while the silver cluster-enhancer alignment is only controlled by the interactions between the NC probe's recognition nucleotide **g** and the nucleotides-of-interest in the targets. Our maNCB design goal is thus to identify a suitable recognition nucleotide for the NC probe that can generate two differentiable silver cluster emission spectra upon probe-target binding.

Received: June 17, 2015
Published: August 11, 2015

DOI: 10.1021/jacs.5b06038
J. Am. Chem. Soc. 2015, 137, 10476−10479

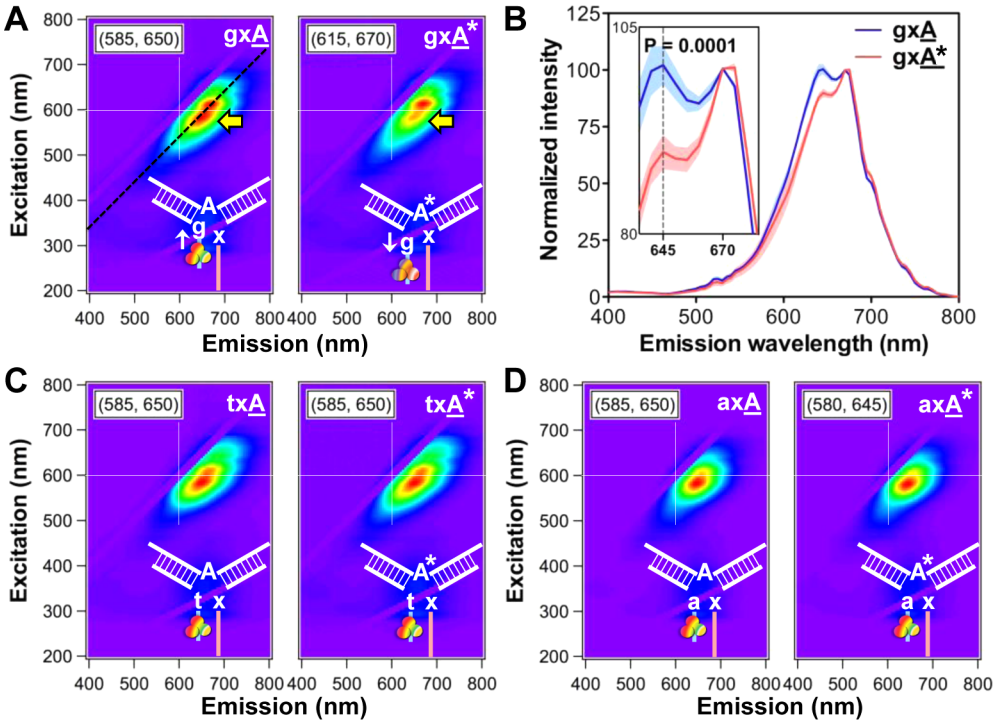

Figure 2. (A) Two-dimensional fluorescence contour plots of **gxA** and **gxA*** that clearly differentiate between A* and A targets (indicated by yellow arrows). The only difference between these two targets (60-nt long) is an A to A* (m^6A) substitution right in the middle of the sequence (Target Set 1 in Table S1). White arrow pointing upward indicates a stronger A−g interaction as compared to A*−g interaction. (B) Emission profiles of **gxA** and **gxA*** (intensity normalized at 670 nm) along the black dash line in panel A (with Stokes shift of 60 nm). Inset shows the zoom-in view of the emission peaks. Error bars (represented by ribbons) show standard deviations from five trials. The P-value is found to be 0.0001 at 645 nm. (C,D) When using **t** or **a** as recognition nucleotides (**txA** vs **txA*** and **axA** vs **axA***), no significant changes in 2D spectra are observed. Target sequence used here has the GATC motif (Target Set 1).

sequence.[21] In other words, the fluorescence emission of silver clusters is sensitive to the nucleobase environment surrounding the clusters. Taking advantage of this fluorescence tunability by altering the surrounding ligands, a property that is not commonly seen among existing reporters,[22,23] NCB soon evolved to a multicolor probe, termed chameleon NanoCluster Beacon (cNCB), for single-nucleotide polymorphism (SNP) detection.[21] Here we bring the NCB detection to the next level by designing a new NCB specifically for m^6A detection.

Similar to cNCB, maNCB adopts a binary probe configuration[24] that forms a 3-way junction (3WJ) with the DNA target (Figure 1). Consisting of an NC probe (i.e., the C-rich Ag cluster-nucleation sequence shown in blue) and an enhancer probe (i.e., the G-rich sequence shown in red), maNCB binds to the target around the "nucleotide-of-interest," which is either m^6A (N^6-methyladenine, denoted as A* in Figure 1) or A (unmethylated adenine) in this study. Since the most common occurrence of m^6A was identified within GATC sites,[25] two 60-nt long targets containing either a GATC or a GA*****TC site were synthesized (Target Set 1 in Table S1). These two targets have exactly identical sequences except for a single-nucleotide substitution (**A** → **A***) in the middle (denoted as the "A target" and the "A* target", respectively, in Figure 1). Upon 3WJ formation between the probe and the target, two "recognition nucleotides" (one on the NC probe and the other on the enhancer probe) are brought close to the nucleotide-of-interest in the target. In the previous SNP detection using cNCB,[21] Watson−Crick basepairing is formed between the nucleotide-of-interest and one of the recognition nucleotides, leading to two distinct alignment states between the silver cluster and the enhancer sequence. Our main task in the maNCB design is therefore to search for a set of recognition nucleotides that can discriminate m^6A from A by distinct emission spectra of activated silver clusters.

We tested all recognition nucleotide combinations but failed to achieve a working maNCB design (Figure S1). In the second attempt, we reduced the number of recognition nucleotides from two to one by introducing an abasic site (denoted as **x** in Figure 1) to the enhancer probe. Out of the four recognition nucleotides tested on the NC probe, we noticed that only **g** could give differentiable silver cluster emission spectra upon probe-target binding (spectrum difference pointed by arrows in Figure 2A). The difference in 2D spectra can be more clearly seen in 1D spectra (Figure 2B), which were plotted along a 45° line (with a fixed Stokes shift of 60 nm) and normalized at 670 nm. The two 1D spectra unambiguously deviated from each other at 645 nm, with P-value about 0.0001. However, when other recognition nucleotides were used, no differentiation was observed (Figure 2C,D). The discrimination given by **g** must be due to different interaction strengths between A−g and A*−g. Dai et al. has previously identified guanine to be the most effective recognition base in their ligation-based method for N^6-methyladenosine detection on a RNA target.[13] In RNA, adenosine can form a sheared, non-Watson−Crick base pair with guanosine, in which three hydrogen bonds are established between the Hoogsteen edge of adenosine and the sugar edge of guanosine (Figure S2).[26] In crowded space between the Hoogsteen and sugar edges,[27] a bulky N^6-methyl group can (1) hinder the H-bond formation between N^6H of adenosine and 2′OH of guanosine and (2) cause steric clash with the phosphate backbone of guanosine.[13] In our case, while the former has no contribution since both our targets

DOI: 10.1021/jacs.5b06038
J. Am. Chem. Soc. 2015, 137, 10476−10479

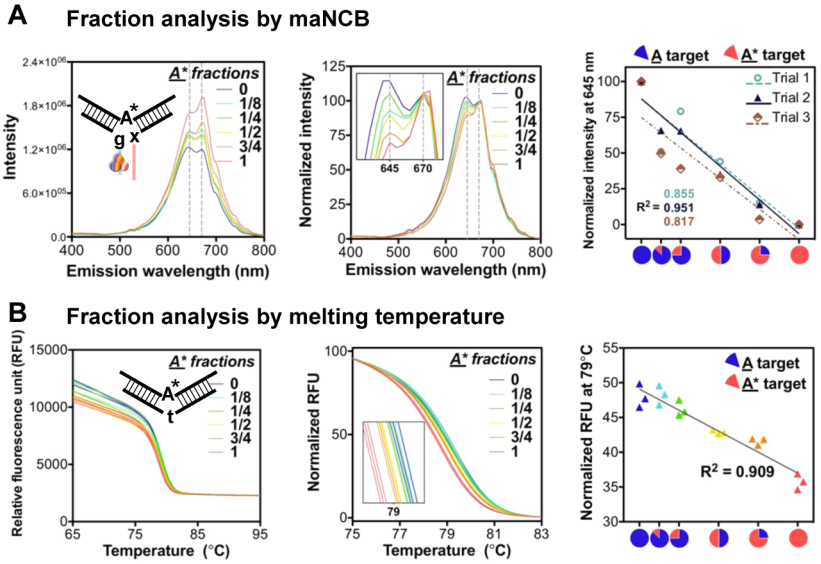

Figure 3. Quantification of adenine methylation extent in heterogeneous samples. (A) Six samples with different A* target fractions (Target Set 1) are prepared and mixed with maNCB_1. Here fraction **0** means 100% A target and fraction **1** means 100% A* target. After normalization at 670 nm, maNCB's emission intensity at 645 nm is found correlated to the amount of A* target in the mixture (R^2 range: 0.817 to 0.951). (B) High-resolution melting analyses are also performed in the six dsDNA mixtures. After normalization at 75 and 83 °C ($T_m \pm 4$ °C), intercalating dye's emission intensity at 79 °C is also found correlated to the amount of A* target in the mixture ($R^2 = 0.909$). Target sequence used here has the GATC motif (Target Set 1).

and probes are DNA, the latter can weaken the Hoogsteen A*−g interaction, resulting in the spectral differences at 645 nm (Figure 2). We also notice that the dsDNA with an A*-g pair in the middle has a melting temperature lower than that of the dsDNA with an A−g pair (Figure S4). While testing the same maNCB design (using **g** as the recognition nucleotide for NC probe) on a second GATC-containing target set[28] (Target Set 2 in Table S1), differentiable spectra, similar to those from Target Set 1, were obtained (Figure S3).

Whereas our first maNCB design worked well for the GATC site, it could not differentiate m^{6}A from A on the CTGCAG site[10,29] (Target Sets 3 and 4 in Table S3). Instead, **t** served as a good recognition nucleotide for NC probe to detect m^{6}A on the CTGCAG sites (Figure S5 and S6). Upon closer examination, we noticed that the resulting spectra from the second maNCB design (where **t** is used as recognition nucleotide) were very different from those obtained from the first maNCB design (where **g** is used as recognition nucleotide). The **gxA** and **gxA*** complexes (from Target Sets 1 and 2) led to two major fluorescent species, which emitted at 645 and 670 nm, respectively (Figures 2B and S3B). Here the differentiation of m^{6}A from A was actually caused by suppression of the 645 nm species relative to the 670 nm species in the **gxA*** complex. However, the **txA** and **txA*** complexes (from Target Sets 3 and 4) produced at least three major species, which emitted at 620, 645, and 670 nm (Figure S5B and S6B). The m^{6}A differentiation here was caused by suppression of the 620 nm species relative to the 670 nm species in the **txA*** complex. While it is not clear why we had two major fluorescent species in one case (with GATC site) and three species in another case (with CTGCAG site), it is obvious that subtle changes in the ligand environment favor the formation of one cluster species over another, enabling the m^{6}A detection through a simple "two-color analysis". In our maNCB detection, the 670 nm emission serves as the normalization standard (Figures 2B, S3B, S5B, and S6B), while the relative intensity at 645 nm (Target Sets 1 and 2) or 620 nm (Target Sets 3 and 4) can differentiate m^{6}A from A. We emphasize that our maNCB detection results are highly reproducible and consistent among targets ($P \ll 0.05$, Table S4).

Taking advantage of the large relative-intensity change at 620/645 nm, maNCB can precisely quantify the degree of methylation in heterogeneous samples. Nucleic acid targets are not always fully modified, where incomplete modification can be due to low availability of the cosubstrates and limited modification enzyme activities.[30] To evaluate maNCB quantification in heterogeneous samples, we mixed A* and A targets at six different ratios and compared the resulting relative intensities at a fixed wavelength (645 nm for Target Set 1 in Figure 3A and 620 nm for Target Set 3 in Figure S7A). As expected, maNCB's relative emission at 645 nm was found proportional to the A* target fraction, demonstrating the quantification of methylation degree in heterogeneous samples by maNCB (Figure 3A). As shown in Figures 3B and S7B (see Table S2 for sequences and Figure S8 for the first derivative plots of the melting curves), high-resolution melting (HRM) analysis can also be used for m^{6}A detection. It was previously shown that A−T pair is more stable than A*−T pair in DNA.[15] Whereas normalized fluorescence intensity of intercalating dye (EvaGreen) also showed a linear trend with A* amount and could be used to quantify the A*/A mixing ratio, the melting analysis cannot "pinpoint" the location of a specific A* modification on the target.

To demonstrate the maNCB's capability of pinpointing the location of a specific m^{6}A, two maNCBs, which targets different adenines in the same target sequence, were designed and tested. As expected, the background-subtracted spectra (Figure 4) clearly indicated that m^{6}A at site 1 can only be detected by maNCB_1 ($P \ll 0.05$ at 645 nm), but not maNCB_5 (Table S1). This "pinpoint specificity" in m^{6}A detection was also preserved in targets with CTGCAG site (Figure S9 and Table S3). Furthermore, this new silver cluster probe has very low background fluorescence (Figure S10) and can detect the A* target at 1 μM concentration (Figure S11).

DOI: 10.1021/jacs.5b06038
J. Am. Chem. Soc. 2015, 137, 10476−10479

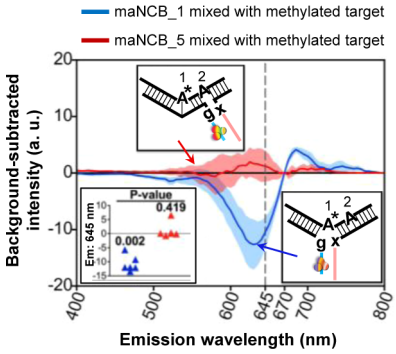

Figure 4. maNCB can pinpoint the location of a specific m^{6}A in the DNA sequence. maNCB_1 is designed to target the adenine within the GATC motif (site 1), while maNCB_5 targets a nearby adenine (site 2). Emission spectra from the unmethylated target−probe mixtures are used as background for subtraction. The background-subtracted spectrum of maNCB_5 (red line) clearly indicates that maNCB_5 cannot detect m^{6}A within the GATC motif, while the background-subtracted maNCB_1 spectrum (blue line) shows an unambiguous detection result of m^{6}A within the GATC motif at 645 nm ($P \approx 0.002$). Error bars (represented by ribbons) show standard deviations from five trials.

In summary, we have demonstrated the use of maNCBs for m^{6}A detection at the single-base resolution. This enzyme-free detection method comes with high reproducibility and can directly quantify the extent of adenine modification at a particular site in heterogeneous samples. To date, there is no hybridization technique that has the potential to reach these remarkable results. We expect that the concept of maNCB can be generally applied to the detection of different types of methylation modifications such as 5-methylcytosine,[31] N^4-methylcytosine,[32] 5-hydroxymethylcytosine,[33] and N^7-methylguanine,[34] as long as the suitable recognition nucleotides are identified in the NCB design.

■ ASSOCIATED CONTENT

Supporting Information

The Supporting Information is available free of charge on the ACS Publications website at DOI: 10.1021/jacs.5b06038.

Detailed preparation of methyladenine-specific Nano-Cluster Beacons (maNCBs), fluorescence measurement procedure, 2D fluorescence contour plots of maNCBs, and high-resolution melting curves (PDF)

■ AUTHOR INFORMATION

Corresponding Author

*tim.yeh@austin.utexas.edu

Author Contributions

†These authors contributed equally to this work.

Notes

The authors declare no competing financial interest.

■ ACKNOWLEDGMENTS

We thank Ning Jenny Jiang for her assistance on melting analysis. This work is financially supported by Robert A. Welch Foundation (F-1833 to H.-C.Y.).

■ REFERENCES

(1) Rozenski, J.; Crain, P. F.; McCloskey, J. A. *Nucleic Acids Res.* **1999**, *27*, 196.
(2) McCloskey, J. A.; Rozenski, J. *Nucleic Acids Res.* **2005**, *33*, D135.
(3) Song, C.-X.; Yi, C.; He, C. *Nat. Biotechnol.* **2012**, *30*, 1107.
(4) Low, D. A.; Weyand, N. J.; Mahan, M. J. *Infect. Immun.* **2001**, *69*, 7197.
(5) Hattman, S. *Biochemistry (Moscow)* **2005**, *70*, 550.
(6) Wion, D.; Casadesús, J. *Nat. Rev. Microbiol.* **2006**, *4*, 183.
(7) Vanyushin, B.; Alexandrushkina, N.; Kirnos, M. *FEBS Lett.* **1988**, *233*, 397.
(8) Marinus, M. G. *Annu. Rev. Genet.* **1987**, *21*, 113.
(9) Flusberg, B. A.; Webster, D. R.; Lee, J. H.; Travers, K. J.; Olivares, E. C.; Clark, T. A.; Korlach, J.; Turner, S. W. *Nat. Methods* **2010**, *7*, 461.
(10) Fang, G.; Munera, D.; Friedman, D. I.; Mandlik, A.; Chao, M. C.; Banerjee, O.; Feng, Z. X.; Losic, B.; Mahajan, M. C.; Jabado, O. J.; Deikus, G.; Clark, T. A.; Luong, K.; Murray, I. A.; Davis, B. M.; Keren-Paz, A.; Chess, A.; Roberts, R. J.; Korlach, J.; Turner, S. W.; Kumar, V.; Waldor, M. K.; Schadt, E. E. *Nat. Biotechnol.* **2013**, *31*, 566.
(11) Kellner, S.; Burhenne, J.; Helm, M. *RNA Biol.* **2010**, *7*, 237.
(12) Dominissini, D.; Moshitch-Moshkovitz, S.; Salmon-Divon, M.; Amariglio, N.; Rechavi, G. *Nat. Protoc.* **2013**, *8*, 176.
(13) Dai, Q.; Fong, R.; Saikia, M.; Stephenson, D.; Yu, Y.-t.; Pan, T.; Piccirilli, J. A. *Nucleic Acids Res.* **2007**, *35*, 6322.
(14) Harcourt, E. M.; Ehrenschwender, T.; Batista, P. J.; Chang, H. Y.; Kool, E. T. *J. Am. Chem. Soc.* **2013**, *135*, 19079.
(15) Rodriguez Lopez, C. M.; Lloyd, A. J.; Leonard, K.; Wilkinson, M. J. *Anal. Chem.* **2012**, *84*, 7336.
(16) Yeh, H.-C.; Sharma, J.; Han, J. J.; Martinez, J. S.; Werner, J. H. *Nano Lett.* **2010**, *10*, 3106.
(17) Yeh, H.-C.; Sharma, J.; Han, J. J.; Martinez, J. S.; Werner, J. H. *IEEE Nanotechnol. Mag.* **2011**, *5*, 28.
(18) Obliosca, J. M.; Babin, M. C.; Liu, C.; Liu, Y.-L.; Chen, Y.-A.; Batson, R. A.; Ganguly, M.; Petty, J. T.; Yeh, H.-C. *ACS Nano* **2014**, *8*, 10150.
(19) Juul, S.; Obliosca, J. M.; Liu, C.; Liu, Y.-L.; Chen, Y.-A.; Imphean, D. M.; Knudsen, B. R.; Ho, Y.-P.; Leong, K. W.; Yeh, H.-C. *Nanoscale* **2015**, *7*, 8332.
(20) Sharma, J.; Yeh, H.-C.; Yoo, H.; Werner, J. H.; Martinez, J. S. *Chem. Commun.* **2010**, *46*, 3280.
(21) Yeh, H.-C.; Sharma, J.; Shih, I.-M.; Vu, D. M.; Martinez, J. S.; Werner, J. H. *J. Am. Chem. Soc.* **2012**, *134*, 11550.
(22) Obliosca, J. M.; Liu, C.; Yeh, H.-C. *Nanoscale* **2013**, *5*, 8443.
(23) Obliosca, J. M.; Liu, C.; Batson, R. A.; Babin, M. C.; Werner, J. H.; Yeh, H.-C. *Biosensors* **2013**, *3*, 185.
(24) Kolpashchikov, D. M. *Chem. Rev.* **2010**, *110*, 4709.
(25) Marinus, M. G.; Casadesus, J. *FEMS Microbiol. Rev.* **2009**, *33*, 488.
(26) Leontis, N. B.; Stombaugh, J.; Westhof, E. *Nucleic Acids Res.* **2002**, *30*, 3497.
(27) Walczak, R.; Carbon, P.; Krol, A. *RNA* **1998**, *4*, 74.
(28) Cooper, K. K.; Mandrell, R. E.; Louie, J. W.; Korlach, J.; Clark, T. A.; Parker, C. T.; Huynh, S.; Chain, P. S.; Ahmed, S.; Carter, M. Q. *BMC Genomics* **2014**, *15*, 17.
(29) Hernday, A.; Krabbe, M.; Braaten, B.; Low, D. *Proc. Natl. Acad. Sci. U. S. A.* **2002**, *99*, 16470.
(30) Saikia, M.; Dai, Q.; Decatur, W. A.; Fournier, M. J.; Piccirilli, J. A.; Pan, T. *RNA* **2006**, *12*, 2025.
(31) Herman, J. G.; Graff, J. R.; Myohanen, S.; Nelkin, B. D.; Baylin, S. B. *Proc. Natl. Acad. Sci. U. S. A.* **1996**, *93*, 9821.
(32) Ehrlich, M.; Gamasosa, M. A.; Carreira, L. H.; Ljungdahl, L. G.; Kuo, K. C.; Gehrke, C. W. *Nucleic Acids Res.* **1985**, *13*, 1399.
(33) Pfeifer, G. P.; Kadam, S.; Jin, S. G. *Epigenet. Chromatin* **2013**, *6*, 10.
(34) Rottman, F.; Shatkin, A. J.; Perry, R. P. *Cell* **1974**, *3*, 197.

DOI: 10.1021/jacs.5b06038
J. Am. Chem. Soc. 2015, 137, 10476−10479